The effect of sweep angle on the limit cycle oscillations of aircraft wings

Seher Eken[*] and Metin Orhan Kaya[a]

*Faculty of Aeronautics and Astronautics, Istanbul Technical University,
Maslak Campus, 34469, Istanbul, Turkey*

Abstract. This study focuses on the limit cycle oscillations (LCOs) of cantilever swept-back wings containing a cubic nonlinearity in an incompressible flow. The governing aeroelastic equations of two degrees-of-freedom swept wings are derived through applying the strip theory and unsteady aerodynamics. In order to apply strip theory, mode shapes of the cantilever beam are used. The harmonic balance method is used to calculate the frequencies of LCOs. Linear flutter analysis is conducted for several values of sweep angles to obtain the flutter boundaries.

Keywords: limit cycle oscillations; sweep angle; harmonic balance method

1. Introduction

Aeroelasticity is a multi-disciplinary field, focusing on the interaction of inertia structural and aerodynamic forces. In classical theories of aeroelasticity, aerodynamic and structural forces are assumed to be linear. The *k* method (*V-g* method) is one of the most popular techniques among the classical approaches, which is based on including a structural (or artificial) damping as an additional parameter in the aeroelastic equations. Another widely used technique for aeroelastic analysis is the *p-k* method which is also known as frequency matching method (Dowell 2004, Wright and Cooper 2007). For several decades, these approaches have been widely used to estimate the flutter speed and frequency of the linear structure. However, they fail to capture the phenomena resulted from structural and aerodynamic nonlinearities.

Aerodynamic nonlinearities are often encountered at transonic speeds or high angles of attack where flow separation occurs. Furthermore, structural nonlinearities are classified as being either distributed or concentrated. In general, distributed structural nonlinearities are governed by elastodynamic deformations that affecting the whole structure. Alternatively, concentrated nonlinearities act locally and they commonly arise from worn hinges of the control surfaces, loose control linkages or associated related to material behavior. For a comprehensive review on this subject, the work of Lee *et al*. (1999) should be addressed diligently.

LCO is the phenomenon that based on the system oscillation with limited amplitude. It occurs

---

*Corresponding author, Ph.D., E-mail: durmazseh@itu.edu.tr
[a]Professor, E-mail: kayam@itu.edu.tr

at higher speeds than the linear flutter speed for airfoils containing a hardening cubic nonlinearity, hence, a nonlinear analysis is required to determine this behavior. The cubic nonlinearity as a concentrated structural nonlinearity for a two-degrees-of-freedom (2-DOF) airfoil was first studied by Woolsten *et al*. (1957). The chaotic behavior of two-dimensional airfoils with cubic pitching stiffness in an incompressible flow is investigated by Zhao and Yang (1990). Moreover O'Neil and Strganac (1998) studied the dynamic response of a rigid wing supported by a cubic nonlinear spring. Most recently, the nonlinear dynamical response of a two-degrees-of-freedom aeroelastic airfoil motion with cubic restoring forces is examined by Liu and Dowell (2004). They detected a secondary bifurcation after the primary Hopf (flutter) bifurcation for a cubic hard spring in the pitch degree-of-freedom. Lee *et al*. (2005) have used the harmonic balance (HB) method to predict LCO frequency and amplitude of motion and Liu *et al*. (2007) studied a two-dimensional airfoil including a cubic spring stiffness placed in an incompressible flow. They employed a new formulation of the harmonic balance method for the aeroelastic airfoil to determine the amplitude and the frequency of the limit cycle oscillations.

Recently, Chen and Liu 2008 are the first to apply homotopy analysis method to solve the flutter system of a two-dimensional airfoil with a cubic structural nonlinearity. In another study Ghadiri and Razi (2007) are investigated LCO and nonlinear aeroelastic analysis of rectangular cantilever wings with hardening and softening cubic nonlinearities. Moreover, for further reading more recent publications by Koohi *et al*. (2014), Chen *et al*. (2012), Shams *et al*. (2012), Peng and Han (2011), Jaworski and Dowell (2009) should be addressed.

Barmby (1950) reported the effects of sweep on the flutter characteristics. He included both experimental and analytical investigations of the flutter of swept-back wings. However, the effects of finite span and compressibility with their relation to sweep are not made. Recently, Marzocca *et al*. (2002) has developed a unified approach of the stability and aeroelastic response of swept aircraft wings. Yet the structural nonlinearity in the aeroelastic analysis of swept-back wings has not been investigated in any of the work mentioned previously. Within this context, in this study we-investigate the effects of sweep angle on the limit cycle oscillations of aircraft wings containing a hardening cubic nonlinearity. For this purpose, the governing aeroelastic equations of a two degrees-of-freedom swept cantilever wing are derived through applying the strip theory using single-mode discretization. The unsteady aerodynamic lift and moment in an incompressible flow are expressed in the time domain by the use of Wagner's functions. The harmonic balance and the Runge-Kutta methods are used to calculate the frequencies of LCO. Besides, to perform LCO analysis linear flutter analysis is at first conducted for several values of sweep angles. The flutter boundaries are obtained and compared with the published studies showing a very good agreement. The finite span effects are also presented to play a significant role in predicting the flutter condition.

2. Analytical developments

2.1 Basic considerations

The airfoil section of the wing swept at an angle of Λ is demonstrated in Fig. 1. As shown, there are two degrees of freedom: plunge deflection and pitch angle represented by *h* and *α*, respectively (Durmaz and Kaya 2012). The distances of mid-chord to elastic axis and elastic axis to center of mass denoted by non-dimensional quantities a_Λ and x_α, respectively. Lastly, semi-
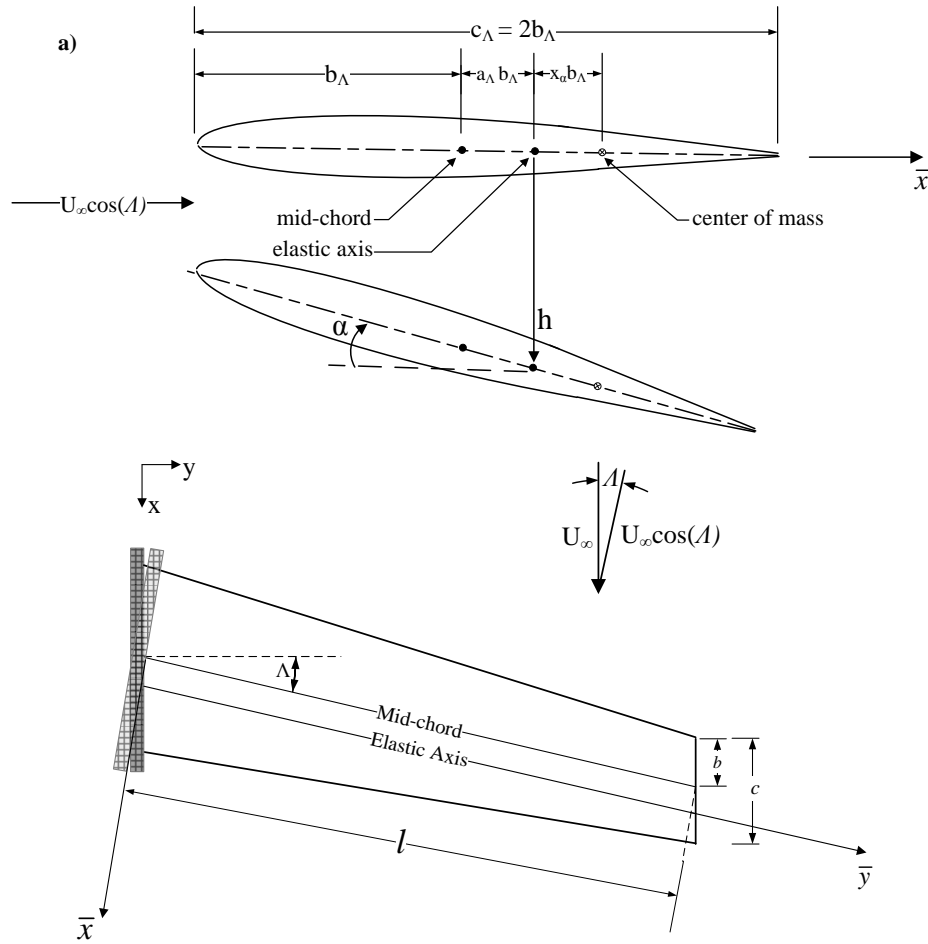
Fig. 1 The sketch of (a) airfoil section (b) wing section

chord of the airfoil is defined by b_Λ and the freestream velocity by U_Λ. The subscript Λ shows that the corresponded quantity is in normal direction to the elastic axis. Next, the planform view of the wing is given in Fig. 2.

Here, l represents the span in $\bar{y}$-direction. In the light of Fig. 1 the position of the centerline of the cross-section could be defined by

$$z(\bar{x},\bar{y},t) = h(\bar{y},t) + \bar{x}\alpha(\bar{y},t) \tag{1}$$

where $\bar{x} = b_\Lambda\left(\frac{1}{2} - a_\Lambda\right)$. Thereby the downwash velocity w normal to the lifting surface is given, for small disturbances, by

$$w(\bar{x},\bar{y},t) = \frac{\partial z}{\partial t} + U_\infty \frac{\partial z}{\partial \bar{x}} \tag{2}$$

For swept wings in an incompressible flow, the downwash velocity is expressed as follows

$$w(\bar{x},\bar{y},\tau)=U_\Lambda\left[\dot{h}/b_\Lambda+\alpha+h'\tan\Lambda+\left(\tfrac{1}{2}-a_\Lambda\right)\left(\dot{\alpha}+b_\Lambda\alpha'\tan\Lambda\right)\right]\tag{3}$$

where ( )′ and (˙) denote the partial differentiation with respect to the reduced time $\tau=U_\Lambda t/b_\Lambda$ and spanwise coordinate along the elastic axis $\bar{y}$. h' and α' are the rates of change of bending and twist in the spanwise direction, respectively.

The total lift per span and pitching moment about elastic axis are expressed by

$$
\begin{aligned}
L_a(\bar{y},\tau)=&\,C_{L_\alpha}\rho U_\Lambda^2 b_\Lambda\phi(\tau)\left[\dot{h}/b_\Lambda+\alpha+\left(\tfrac{1}{2}-a_\Lambda\right)\left[\dot{\alpha}+b_\Lambda\alpha'\tan\Lambda\right]\right]_{\tau=0}\\
&-C_{L_\alpha}\rho U_\Lambda^2 b_\Lambda\int_0^\tau\phi(\tau-\sigma)\left[\ddot{h}/b_\Lambda+\dot{\alpha}+\dot{h}'\tan\Lambda+\left(\tfrac{1}{2}-a_\Lambda\right)\left[\ddot{\alpha}+b_\Lambda\dot{\alpha}\tan\Lambda\right]\right]d\sigma\\
&-\tfrac{1}{2}C_{L_\alpha}\rho U_\Lambda^2 b_\Lambda\left[\ddot{h}/b_\Lambda+\dot{\alpha}+2\dot{h}'\tan\Lambda+b_\Lambda\alpha\tan\Lambda+b_\Lambda h''\tan^2\Lambda\right]\\
&+\tfrac{1}{2}C_{L_\alpha}\rho U_\Lambda^2 b_\Lambda a_\Lambda\left[\ddot{\alpha}+2b_\Lambda\dot{\alpha}'\tan\Lambda+b_\Lambda^2\alpha''\tan^2\Lambda\right]
\end{aligned}\tag{4}
$$

$$
\begin{aligned}
M_a(\bar{y},\tau)=&-C_{L_\alpha}\rho U_\Lambda^2 b_\Lambda\left(\tfrac{1}{2}+a_\Lambda\right)\phi(\tau)\left[\dot{h}/b_\Lambda+\alpha+\left(\tfrac{1}{2}-a_\Lambda\right)\left[\dot{\alpha}+b_\Lambda\alpha'\tan\Lambda\right]\right]_{\tau=0}\\
&+C_{L_\alpha}\rho U_\Lambda^2 b_\Lambda\left(\tfrac{1}{2}+a_\Lambda\right)\int_0^\tau\phi(\tau-\sigma)\left[\ddot{h}/b_\Lambda+\dot{\alpha}+\dot{h}'\tan\Lambda+\left(\tfrac{1}{2}-a_\Lambda\right)\left[\ddot{\alpha}+b_\Lambda\dot{\alpha}'\tan\Lambda\right]\right]d\sigma\\
&+\tfrac{1}{2}C_{L_\alpha}\rho U_\Lambda^2 b_\Lambda a_\Lambda\left[\ddot{h}/b_\Lambda+2\dot{h}'\tan\Lambda+b_\Lambda\alpha'\tan\Lambda+b_\Lambda h''\tan^2\Lambda\right]\\
&-\tfrac{1}{2}C_{L_\alpha}\rho U_\Lambda^2 b_\Lambda^2\left(\tfrac{1}{8}+a_\Lambda^2\right)\left[\ddot{\alpha}+2b_\Lambda\dot{\alpha}'\tan\Lambda+b_\Lambda^2\alpha''\tan^2\Lambda\right]\\
&-\tfrac{1}{2}C_{L_\alpha}\rho U_\Lambda^2 b_\Lambda^2\left[\left(\tfrac{1}{2}-a_\Lambda\right)\dot{\alpha}+\tfrac{1}{2}b_\Lambda\alpha'\tan\Lambda\right]
\end{aligned}\tag{5}
$$

where $\phi(\tau)$ denotes Wagner's function[15] which is expressed as

$$\phi(\tau)=1-\psi_1 e^{-\varepsilon_1\tau}-\psi_2 e^{-\varepsilon_2\tau}\tag{6}$$

in which $\psi_1=0.165$; $\psi_2=0.335$; $\varepsilon_1=0.0455$ and $\varepsilon_2=0.3$.

2.2 Aeroelastic equations

The governing aeroelastic equations of wing oscillating in pitch and plunge are derived using Euler-Lagrange relations which are expressed as

$$\frac{d}{d\tau}\left(\frac{\partial T}{\partial\dot{h}}\right)-\frac{\partial T}{\partial h}+\frac{\partial V}{\partial h}+\frac{\partial D}{\partial h}=Q_h\tag{7}$$

$$\frac{d}{d\tau}\left(\frac{\partial T}{\partial\dot{\alpha}}\right)-\frac{\partial T}{\partial\alpha}+\frac{\partial V}{\partial\alpha}+\frac{\partial D}{\partial\alpha}=Q_\alpha\tag{8}$$

Here kinetic, potential and damping energy expressions are given below.

$$T = \frac{1}{2}\int_0^l \left[m(\dot{h} + b_\Lambda x_\alpha \dot{\alpha})^2 + I_{CG}(\dot{\alpha})^2 \right] d\bar{y} \tag{9}$$

$$V = \frac{1}{2}\int_0^l \left[EI(h'')^2 + GJ(\alpha')^2 \right] d\bar{y} \tag{10}$$

$$D = \frac{1}{2}\int_0^l \left[C_h(\dot{h})^2 + C_\alpha(\dot{\alpha})^2 \right] d\bar{y} \tag{11}$$

where *EI* and *GJ* are the bending and torsional stiffnesses of the uniform cantilever beam while C_h and C_α are the corresponding damping coefficients. *m* and I_{CG} represent mass per unit length and wing mass moment of inertia per unit length (about center of gravity). Moreover the generalized force terms Q_h and Q_α in Eqs. (7) and (8) will be expressed in the following sections.

The decoupled eigenmodes in pitch and plunge motion are expressed for the cantilever wing in the following form (Hodges and Pierce 2011)

$$\phi_h(\eta) = \left(\frac{\sinh\beta_1 + \sin\beta_1}{\cosh\beta_1 + \cos\beta_1} \right)[\cos(\beta_1\eta) - \cosh(\beta_1\eta)] + \sinh(\beta_1\eta) - \sin(\beta_1\eta) \tag{12}$$

$$\phi_\alpha(\eta) = \sin(\beta_2\eta) \tag{13}$$

where $\eta = \bar{y}/l$, $\beta_1 = 0.5969\pi$ and $\beta_2 = 0.5\pi$.

Assuming separation of variables and using single mode discretization the plunge deflection and the pitch angle are expressed in terms of time-dependent parts. The assumed mode shapes given in Eqs. (12) and (13).

$$h(\eta, t) = \phi_h(\eta)\bar{h}(t) \tag{14}$$

$$\alpha(\eta, t) = \phi_\alpha(\eta)\bar{\alpha}(t) \tag{15}$$

From now on, dropping the bar, the time mode of plunge displacement and pitch angle is written as *h*(*t*) and *α*(*t*), respectively. The kinetic, potential and damping energy expressions are rewritten by substituting Eqs. (14) and (15) into (9)-(10). Consequently, using Euler-Lagrange relations

$$c_3\ddot{\xi} + c_5 x_\alpha \ddot{\alpha} + c_3\zeta_\xi\left(\frac{\bar{\omega}}{U_\Lambda^*}\right)\dot{\xi} + c_3\left(\frac{\bar{\omega}}{U_\Lambda^*}\right)^2 G_\xi(\xi) = \frac{b_\Lambda}{mlU_\Lambda^2}Q_h \tag{16}$$

$$c_5\frac{x_\alpha}{r_\alpha^2}\ddot{\xi} + c_4\ddot{\alpha} + c_4\zeta_\alpha\left(\frac{1}{U_\Lambda^*}\right)\dot{\alpha} + c_4\left(\frac{1}{U_\Lambda^*}\right)^2 G_\alpha(\alpha) = \frac{b_\Lambda^2}{I_\alpha mlU_\Lambda^2}Q_\alpha \tag{17}$$

where $G_\xi(\xi) = \beta_\xi\xi + \gamma_\xi\xi^3$ and $G_\alpha(\alpha) = \beta_\alpha\alpha + \gamma_\alpha\alpha^3$. These functions are selected to represent the structural nonlinearities in plunge and pitch motion, respectively. Note that β_ξ, β_α, γ_ξ and γ_α are the constant coefficients. All of the non-dimensional quantities that are used to obtain the Eqs. (16) and (17) are given in the following.

$$\xi = h/b_\Lambda \qquad \mu = m/\left(\pi\rho b_\Lambda^2\right) \qquad r_\alpha = \sqrt{I_\alpha/\left(m\,b_\Lambda^2\right)}$$

$$U_\Lambda = U_\Lambda /(m\omega_\alpha) \qquad \overline{\omega} = \omega_h/\omega_\alpha \qquad \omega_h = \sqrt{c_1 EI/\left(c_3 ml^4\right)}$$

$$\omega_\alpha = \sqrt{c_2 GJ/\left(c_4 I_\alpha l^4\right)} \qquad \xi_\xi = l^2 C_h \sqrt{(c_3/c_1 mEI)} \qquad \xi_\alpha = lC_\alpha \sqrt{c_2/\left(c_4 I_\alpha GJ\right)}$$

Here, ω_h and ω_α are the fundamental frequency of plunging and pitching modes, ζ_ξ and ζ_α are the viscous damping ratios in plunge and pitch, and also U_Λ, μ and r_α are the non-dimensional freestream speed, mass ratio and radius of gyration about the elastic axis, respectively. Additionally, the constants $c_1, c_2,..., c_{12}$ are described in Appendix A.

2.3 Force and moment expressions

The generalized force terms Q_h and Q_α in the right hand sides of the Eqs. (7) and (8) are derived by virtual work law and expressed as (Gulcat 2010)

$$Q_h = l\int_0^1 L_a(y',t)\phi_h(\eta)d\eta \tag{18a}$$

$$Q_\alpha = l\int_0^1 M_a(y',t)\phi_\alpha(\eta)d\eta \tag{18b}$$

Inserting the Eqs. (4) and (5) into (18) and carrying out the integration, we have

$$
\begin{aligned}
Q_h &= C_{L_\alpha}\rho U_\Lambda^2 b_\Lambda l\phi(\tau)\left[c_3\dot\xi + c_5\alpha + \left(\tfrac{1}{2}-a_\Lambda\right)\left[c_5\dot\alpha + c_7\alpha \tan\Lambda\right]\right]_{\tau=0} \\
&\quad - C_{L_\alpha}\rho U_\Lambda^2 b_\Lambda l\int_0^\tau \phi(\tau-\sigma)\left[c_3\ddot\xi + c_5\dot\alpha + c_6\xi \tan\Lambda + \left(\tfrac{1}{2}-a_\Lambda\right)\left[c_5\ddot\alpha + c_7\dot\alpha \tan\Lambda\right]\right]d\sigma \\
&\quad - \tfrac{1}{2}C_{L_\alpha}\rho U_\Lambda^2 b_\Lambda l\left[c_3\ddot\xi + c_5\dot\alpha + 2c_6\dot\xi \tan\Lambda + c_7\alpha \tan\Lambda + c_8\,\ddot\xi\tan^2\Lambda\right] \\
&\quad + \tfrac{1}{2}C_{L_\alpha}\rho U_\Lambda^2 b_\Lambda a_\Lambda l\left[c_5\ddot\alpha + 2c_7\alpha \tan\Lambda + c_9\alpha \tan^2\Lambda\right]
\end{aligned}
\tag{19}
$$

$$
\begin{aligned}
Q_\alpha &= -C_{L_\alpha}\rho U_\Lambda^2 b_\Lambda\left(\tfrac{1}{2}+a_\Lambda\right)l\phi(\tau)\left[c_5\dot\xi + c_4\alpha + \left(\tfrac{1}{2}-a_\Lambda\right)\left[c_4\dot\alpha + c_{11}\alpha \tan\Lambda\right]\right]_{\tau=0} \\
&\quad + C_{L_\alpha}\rho U_\Lambda^2 b_\Lambda\left(\tfrac{1}{2}+a_\Lambda\right)l\int_0^\tau \phi(\tau-\sigma)\left[c_5\ddot\xi + c_4\dot\alpha + c_{10}\dot\xi \tan\Lambda + \left(\tfrac{1}{2}-a_\Lambda\right)\left[c_4\ddot\alpha + c_{11}\dot\alpha \tan\Lambda\right]\right]d\sigma \\
&\quad + \tfrac{1}{2}C_{L_\alpha}\rho U_\Lambda^2 b_\Lambda a_\Lambda l\left[c_5\ddot\xi + 2c_{10}\dot\xi \tan\Lambda + c_{11}\alpha' \tan\Lambda + c_{12}\xi \tan^2\Lambda\right] \\
&\quad - \tfrac{1}{2}C_{L_\alpha}\rho U_\Lambda^2 b_\Lambda^2\left(\tfrac{1}{8}+a_\Lambda^2\right)l\left[c_4\ddot\alpha + 2c_{11}\dot\alpha \tan\Lambda + c_{13}\alpha \tan^2\Lambda\right] \\
&\quad - \tfrac{1}{2}C_{L_\alpha}\rho U_\Lambda^2 b_\Lambda^2 l\left[c_4\left(\tfrac{1}{2}-a_\Lambda\right)\dot\alpha + \tfrac{1}{2}c_{11}\alpha \tan\Lambda\right]
\end{aligned}
\tag{20}
$$

Substituting Eqs. (19) and (20) into Eqs. (16) and (17), an integro-differential equation is obtained. Therefore the governing aeroelastic equations of a rectangular swept-back wing are obtained as

$$a_1\ddot{\xi} + a_2\ddot{\alpha} + a_3\dot{\xi} + a_4\dot{\alpha} + a_5\xi + a_6\alpha + a_7w_1 + a_8w_2 + a_9w_3 + a_{10}w_4 + a_{11}G_\xi(\xi) = a_{12}\dot{\phi}(\tau) \qquad (21)$$

$$b_1\ddot{\xi} + b_2\ddot{\alpha} + b_3\dot{\xi} + b_4\dot{\alpha} + b_5\xi + b_6\alpha + b_7w_1 + b_8w_2 + b_9w_3 + b_{10}w_4 + b_{11}G_\alpha(\alpha) = b_{12}\dot{\phi}(\tau) \qquad (22)$$

Recall that $G_\xi(\xi)=\beta_\xi\xi+\gamma_\xi\xi^3$ and $G_\alpha(\alpha)=\beta_\alpha\alpha+\gamma_\alpha\alpha^3$. Also, four new functions $w_1(\tau)$, $w_2(\tau)$, $w_3(\tau)$ and $w_4(\tau)$ are determined for the sake of simplicity to so lve the integro-differential equation. These are described by the following integrals (Lee *et al*. 1997)

$$w_1(\tau) = \int_0^\tau e^{-\varepsilon_1(\tau-\sigma)}\alpha(\sigma)d\sigma \qquad (23a)$$

$$w_2(\tau) = \int_0^\tau e^{-\varepsilon_2(\tau-\sigma)}\alpha(\sigma)d\sigma \qquad (23b)$$

$$w_3(\tau) = \int_0^\tau e^{-\varepsilon_1(\tau-\sigma)}\xi(\sigma)d\sigma \qquad (23c)$$

$$w_4(\tau) = \int_0^\tau e^{-\varepsilon_2(\tau-\sigma)}\xi(\sigma)d\sigma \qquad (23d)$$

The coefficients a_1, a_2,..., a_{12} and b_1, b_2,..., b_{12} appear in Eqs. (21) and (22) are also given in Appendix A.

3. Solution procedures

3.1 Harmonic balance method

The method of harmonic balance corresponds to a truncated Fourier series and allows systematic determination of the coefficients to the various harmonics and the angular frequency (Mickens 2010). In order to apply this method, plunge and pitch motions are assumed as a trigonometric series as follows

$$\xi(\tau) = \sum_{i=3,5,...} f_i \sin(i\omega\tau) + g_i \cos(i\omega\tau) \qquad (24)$$

$$\alpha(\tau) = d_1 \cos(\omega\tau) + \sum_{n=3,5,...} c_n \sin(n\omega\tau) + d_n \cos(n\omega\tau) \qquad (25)$$

For a detailed review of the method the study of Lee *et al*. (1997) should be addressed. Besides, similar to the harmonic balance method the homotopy analysis method could also be applied to obtain the nonlinear frequency of the system. For this method, the author's previous work (Durmaz

et al. 2011) and the study by Zhao *et al*. (2014), Chen and Liu (2008) should be carefully reviewed.

3.2 Numerical solution

The numerical solution is handled by standard fourth-order Runge-Kutta method. Therefore the governing aeroelastic equations expressed in Eqs. (21) and (22), are rewritten as a set of first order ODEs

$$\frac{dX}{d\tau} = F(x, \tau) \tag{26}$$

where

$$X = \begin{bmatrix} x_1 & x_2 & x_3 & x_4 & x_5 & x_6 & x_7 & x_8 \end{bmatrix}^T = \begin{bmatrix} \xi & \dot{\xi} & \alpha & \dot{\alpha} & w_1 & w_2 & w_3 & w_4 \end{bmatrix}^T \tag{27}$$

and

$$F(x, \tau) = \begin{bmatrix} x_2 \\ -k_1 x_2 - k_2 x_4 - k_3 x_1 - k_4 x_3 - k_5 x_5 - k_6 x_6 - k_7 x_7 - k_8 x_8 - k_9 F_{x_1}(x_1) + k_{10}\phi(\tau) \\ x_4 \\ -m_1 x_2 - m_2 x_4 - m_3 x_1 - m_4 x_3 - m_5 x_5 - m_6 x_6 - m_7 x_7 - m_8 x_8 - m_9 F_{x_3}(x_3) + m_{10}\phi(\tau) \\ x_3 - \varepsilon_1 x_5 \\ x_3 - \varepsilon_2 x_6 \\ x_1 - \varepsilon_1 x_7 \\ x_1 - \varepsilon_2 x_8 \end{bmatrix} \tag{28}$$

The initial conditions of the system are given below

$$X = \begin{bmatrix} x_1(0) & x_2(0) & x_3(0) & x_4(0) & 0 & 0 & 0 & 0 \end{bmatrix}^T \tag{29}$$

The coefficients $k_1, k_2,..., k_{10}$ and $m_1, m_2,..., m_{10}$ are described in Appendix B.

4. Results & discussion

4.1 Linear analysis

To determine the flutter boundaries, linear flutter analysis of a swept-back wing is carried out for the initial conditions set to $\alpha(0)=1°$ and $\xi(0)=\xi'(0)=\alpha'(0)=0$. Stiffness terms are taken as $G_\xi(\xi)=\beta_\xi\xi$ and $G_\alpha(\alpha)=\beta_\alpha\alpha$. The experimental results of the report written by Barmby (1950) are used to validate the proposed swept wing model. Geometrical properties and characteristics of the wing can be found in Table 1.

Linear flutter speeds are calculated for several sweep angles and compared with the experimental results given in Table 2. Noting that the dimensional linear flutter speeds U are computed from non-dimensional speeds $U_{\Lambda L}$ which are given in the second column of Table 2. It is observed that for higher angles of sweep, higher flutter speeds are obtained. Initially, the flutter speeds are calculated by ignoring the thickness of the airfoil, namely taking $C_{L_\alpha} = 2\pi$. As seen the

Table 1 Wing geometry and characteristics

$\beta_\xi=1$	$\mu=37.8$
$\gamma_\xi=0$	$x_\alpha=0.120$
$\beta_\alpha=1$	$r_\alpha=0.526$
$\gamma_\alpha=3$	$\overline{\omega}=0.136$
$a=-0.2$	$\zeta_\xi=\zeta_\alpha=0$

Table 2 Comparison of linear flutter speeds

Λ	U_Λ	U by Barmby (1950)	U^1	U^2
0°	3.64	102.372 m/s	95.7447 m/s	103.422 m/s
30°	3.73	105.054 m/s	96.1668 m/s	104.908 m/s
45°	4.32	121.595 m/s	108.972 m/s	121.046 m/s
60°	5.56	156.464 m/s	136.243 m/s	156.057 m/s

$U_\Lambda = U/(b\omega_\alpha)$
[1] $C_{L_\alpha}=2\pi$, [2] $C_{L_\alpha}=C_{L_\alpha}^{3D}$

results represented by U^1 have relatively smaller values than the experimental speeds besides for higher angles of sweep the difference between them is getting more significant. Therefore the linear flutter speeds are recalculated to include three-dimensional effects. To capture these effects the lift curve slope is expressed by involving the corrections to the aspect ratio and sweep angle Λ and given as (Bislinghoff *et al.* 1975, Flax 1961)

$$C_{L_\alpha}^{3D} = \frac{C_{L_\alpha} AR}{C_{L_\alpha}\cos\Lambda\big/\pi + AR\sqrt{1+\left[C_{L_\alpha}\cos\Lambda/(\pi AR)\right]^2}}$$

where the aspect ratio denoted by *AR* is expressed as

$$AR = l_\Lambda\cos^2\Lambda\big/b_\Lambda$$

Table 2 shows that much better results of the flutter speeds U^2 are obtained by the modification of the lift-curve slope for all sweep configurations. Hence, the effect of sweep angle on the LCOs are investigated and all of the computations are made by considering the corrected expression of C_{L_α} (Durmaz and Kaya 2012).

The variation of the linear flutter speed with respect to sweep angle is investigated and shown in Fig. 2. It is seen that up to sweep angle of 15°, the flutter speeds are decreasing; thereafter speeds are increasing with the sweep angle. Moreover, the difference between the dashed lines and solid lines demonstrates the refinement in flutter speeds made by including three-dimensional effects.

4.2 Nonlinear analysis

In this section nonlinear aeroelastic analysis is performed for the same rectangular swept-back wing. A hardening cubic nonlinearity is only considered in pitch motion by setting $G_\alpha(\alpha)=\beta_\alpha\alpha+\gamma_\alpha\alpha^3$ and $G_\xi(\xi)=\beta_\xi\xi$. It is observed that LCO occurs at speeds higher than the linear flutter speed.
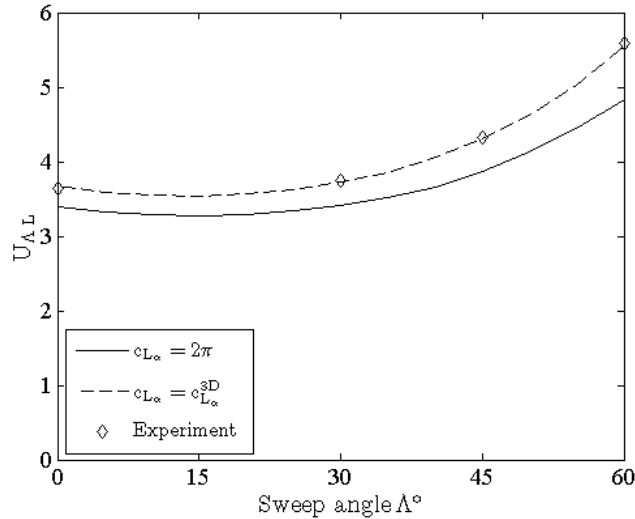
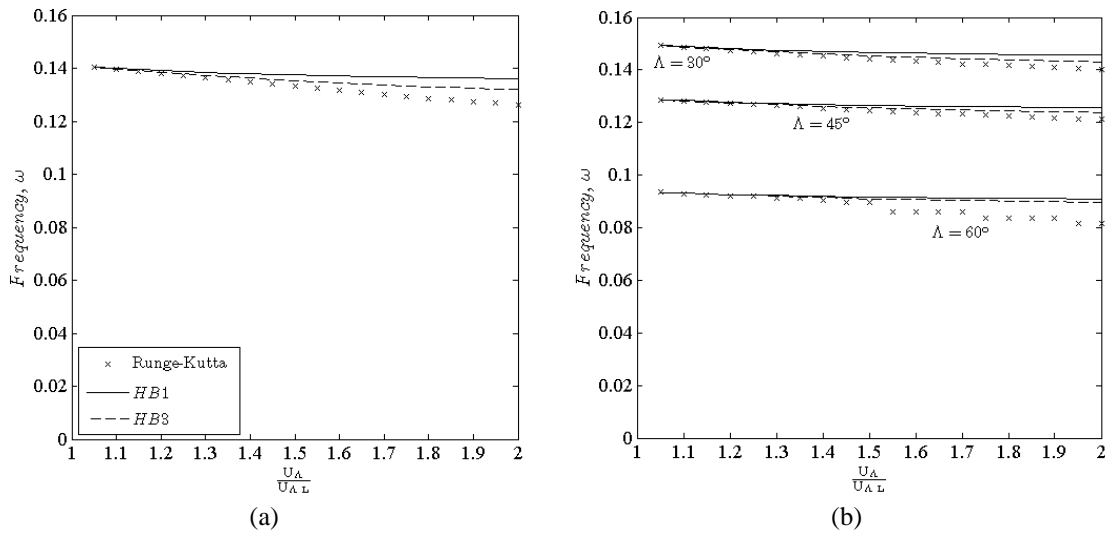Fig. 2 Variation of linear flutter speeds versus sweep angle

(a)	(b)

Fig. 3 Comparison of frequencies of LCO for (a) $\Lambda=0°$, (b) $\Lambda=30°$, $45°$ and $60°$

The frequencies of LCOs are computed for $U_\Lambda/U_{\Lambda L}$ varying from 1.02 to 2 and compared with the numerical solution (RK4). Fig. 3(a) shows the variation of frequencies for the straight wing configuration, similarly Fig. 3(b) shows the same behavior for the sweep angles of 30°, 45° and 60°. It is revealed from both figures that the frequencies of LCOs tend to decrease for increasing values of sweep angles.

In Fig. 3(b), jump phenomena are detected for the sweep configuration of 60° at $U_\Lambda/U_{\Lambda L}$=1.55 and $U_\Lambda/U_{\Lambda L}$=1.75. It is seen that the harmonic balance method generally fails to capture this jump phenomenon.

In Fig. 4(a)-(d), the phase portraits of pitch motion are drawn at $U_\Lambda/U_{\Lambda L}$=1.0, 15, 2.0, 2.5 for

the sweep angles of 0°, 30°, 45° and 60°. As seen from these subfigures, for Λ=0° and Λ=30° all plots are symmetric at different speed ratios. However this trend is not observed for Λ=45° and Λ=60° at speed ratio $U_\Lambda/U_{\Lambda L}$=2.5. Besides, the amplitudes of the LCOs are increasing with the sweep angles.

(a)   (b)
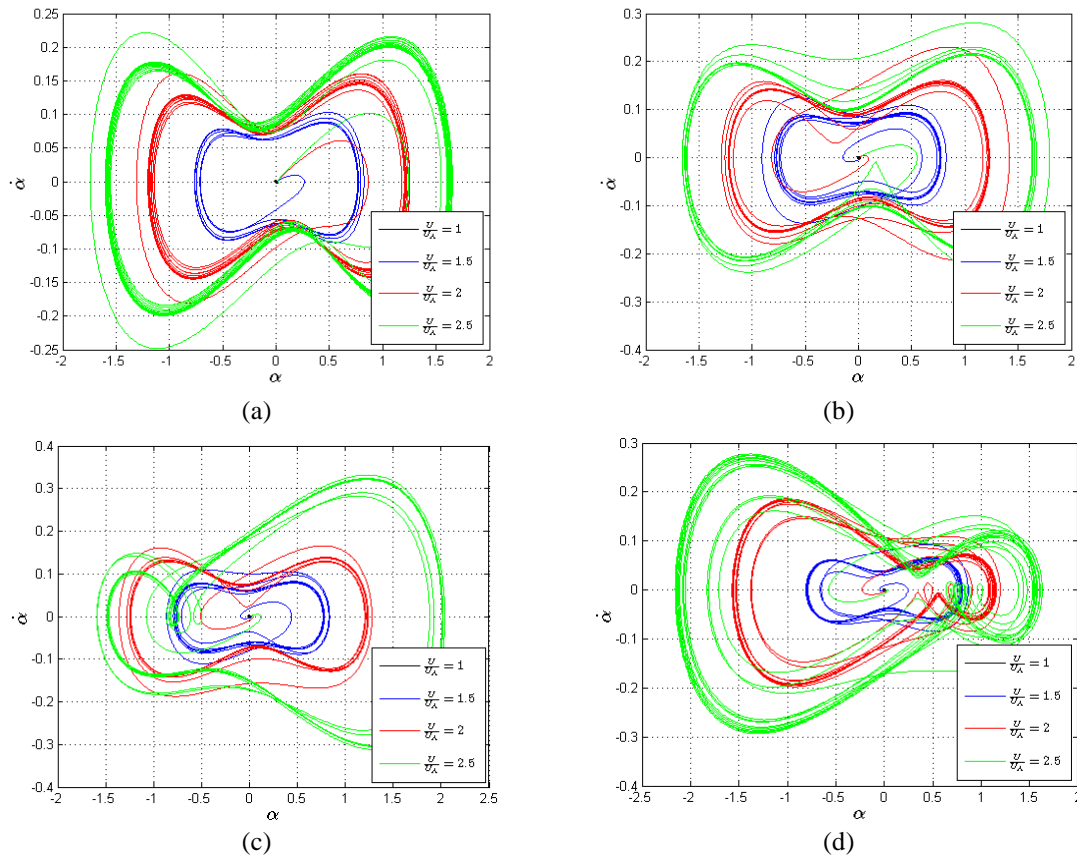

(c)   (d)

Fig. 4 Phase plots for (a) Λ=0º, (b) Λ=30º, (c) Λ=45º and (d) Λ=60º
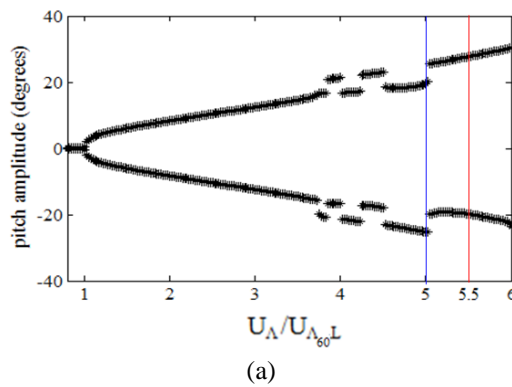

(a)

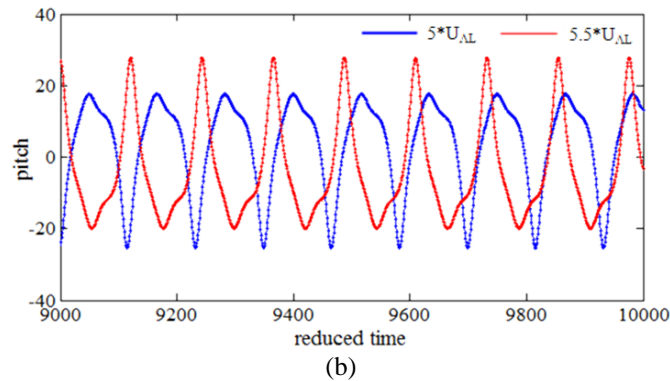Fig. 5 (a) Bifurcation diagram of pitch oscillations (b) Pitch amplitude vs. reduced time for Λ=60º

(b)

Fig. 5 Continued

Fig. 5 shows two plots of pitch degree-of-freedom for sweep angle of 60°. The first subplot, Fig. 5(a) demonstrates the bifurcation diagram. From this figure it is clearly observed that for speed ratios approximately less than 3.7 the equilibrium position remains unchanged and it is at zero. However for higher speed ratios than 3.7, the equilibrium postion alters to a negative or positive value. Regarding this alternation, Fig. 5(b) is plotted for the values of speed ratios which are marked with blue and red lines. As seen from this figure, the pitch oscillations fluctuate at an equilibrium position altering between negative and positive values. For similar phenomenon, the readers should adress to the publication published by Daochun and Jinwu (2008).

5. Conclusions

In this study we analyzed the limit cycle oscillations of swept-back aircraft wings containing a hardening cubic nonlinearity. The unsteady aerodynamic lift and moment in an incompressible flow are expressed in the time domain by the use of Wagner's functions. The aeroelastic equations are solved by the harmonic balance and the Runge-Kutta methods, and the frequencies of LCO are computed and plotted. The effect of the sweep angle on the LCO are examined and concluded that for larger sweep angles the equlibrium position of the response of the wing does not stay stable at zero, instead it alters between negative and positive values. Another outcome is that the accurate prediction of the flutter higly depends on the inclusion of finite-span effects for swept arcraft wings.

References

Barmby, J.C. (1950), "Study of effects of sweep on the flutter of cantilever wings", Eds. Cunningham, H. J. and Garrick, I. E., NACA-Report TN 2121.
Bisplinghoff, R.L. and Ashley, H. (1975), *Principles of Aeroelasticity,* Dover, New York, NY, USA.
Chen, Y.M. and Liu, J.K. (2008), "Homotopy analysis method for limit cycle flutter of airfoils", *Appl. Math. Comput.*, **203**, 854-863.
Chen, Y.M., Liu, J.K. and Meng, G. (2012), "Incremental harmonic balance method for nonlinear flutter of an airfoil with uncertain-but-bounded parameters", *Appl. Math. Model.*, **36** 657-667.

Dowell, E.H. (2004), *A Modern Course in Aeroelasticity*, Springer, The Netherlands.

Daochun, L. and Jinwu, X. (2008), "Chaotic motions of an airfoil with cubic nonlinearity in subsonic flow", *J. Aircraf.*, **45**(4), 1457-1460.

Durmaz, S. and Kaya, M.O. (2012), "Limit cycle oscillations of swept-back wings in an incompressible flow", *AIAA/53rd Structures, Structural Dynamics, and Materials Conference*, Honolulu-Hawaii-USA, April.

Durmaz, S., Kerki, T. and Kaya, M.O. (2011), "Approximate analytical solutions of nonlinear flutter of aircraft wings", *IFASD, 15th International Forum on Aeroelasticity and Structural Dynamics*, Paris, France, June.

Flax, A.H. (1961), *Aeroelasticity and Flutter in High Speed Problems of Aircraft and Experimental Methods Vol. VIII High Speed Aerodynamic and Jet Propulsion*, Eds. Donovan, H.F. and Lawrence, H.R., Princeton University Press.

Ghadiri, B. and Razi, M. (2007), "Limit cycle oscillations of rectangular cantilever wings containing cubic nonlinearity in an incompressible flow", *J. Fluid. Struct.*, **23**(4), 665-680.

Gulcat, U. (2010), *Fundamentals of Modern Unsteady Aerodynamics*, Springer, Berlin, Germany.

Hodges, D.H. and Pierce, G.A. (2011), *Introduction to structural dynamics and aeroelasticity*, Cambridge aerospace series, Cambridge, United Kingdom.

Jaworski, J.W. and Dowell, E. (2009), "Comparison of theoretical structural models with experiment for a high-aspect-ratio aeroelastic wing", *J. Aircraf.*, **46**(2), 708-13.

Koohi, R., Shahverdi, H. and Haddadpour, H. (2014), "Nonlinear aeroelastic analysis of a composite wing by finite element method", *Compos. Struct.*, **113**, 118-126.

Lee, B.H.K., Gong, L. and Wong, Y.S. (1997), "Analysis and computation of nonlinear dynamic response of a two-degree-of freedom system and its application in aeroelasticity", *J. Fluid. Struct.*, **11**(3), 225-246.

Lee, B.H.K., Liu, L. and Chung, K.W. (2005), "Airfoil motion in subsonic flow with strong cubic nonlinear restoring forces", *J. Sound. Vib.*, **281**(3), 699-717.

Lee, B.H.K., Price, S.J. and Wong, Y.C. (1999), "Nonlinear aeroelastic analysis of airfoils: bifurcation and chaos", *Prog. Aerospace Sci.*, **35**(3), 205-334.

Liu, L. and Dowell, E.H. (2004), "The secondary bifurcation of an aeroelastic airfoil motion: effect of high harmonics", *Nonlin. Dyn.,* **37**, 31-49.

Liu, L., Dowell, E.H. and Thomas, J.P. (2007), "A high dimensional harmonic balance approach for an aeroelastic airfoil with cubic restoring forces", *J. Fluid. Struct.*, **23**(3), 351-363.

Marzocca, P., Librescu, L. and Silva, W.A. (2002), "Aeroelastic response and flutter of swept aircraft wings", *AIAA J.*, **40**(5), 801-812.

Mickens, R.E. (2010), *Truly nonlinear oscillations: harmonic balance, parameter expansions, iteration, and averaging methods*, World Scientific Publishing, Danvers, MA, USA.

O'Neil, T. and Strganac, T.W. (1998), "Aeroelastic response of a rigid wing supported by nonlinear springs", *J. Aircraf.*, **35**(4), 616-622.

Peng, C. and Han, J. (2011), "Numerical investigation of the effects of structural geometric and material nonlinearities on limit-cycle oscillation of a cropped delta wing", *J. Fluid. Struct.*, **27**(4), 611-622.

Shams, S., Sadr-Lahidji, M.H. and Haddadpour, H. (2012), "An efficient method for nonlinear aeroelasticy of slender wings", *Nonlin. Dyn.*, **67**, 659-81.

Wright, J.R. and Cooper, J.E. (2007), *Introduction to Aircraft Aeroelasticity and Loads*, Wiley, England.

Woolsten, D.S., Runyan, H.L. and Andrews, R. (1957), "An investigation of effects of certain types of structural nonlinearities on wing and control surface flutter", *J. Aeronaut. Sci.*, **24**(1), 57-63.

Zhao, L.C. and Yang, Z.C. (1990), "Chaotic motions of an airfoil with nonlinear stiffness in incompressible flow", *J. Sound. Vib.*, **138**(2), 245-254.

Zhao, Y., Sun, C., Wang, Z. and Peng, J. (2014), "Nonlinear in-plane free oscillations of suspended cable investigated by homotopy analysis method", *Struct. Eng. Mech.*, **50**(4), 487-500.

CC

Nomenclature

a_Λ	non-dimensional distance from wing section mid-chord to elastic axis
AR	aspect ratio
b_Λ	wing section semi-chord normal to the elastic axis
C_h, C_α	damping coefficients in plunge and pitch
EI	bending stiffness
I_α	mass moment of inertia about elastic axis
G_ξ, G_α	functions correspond to structural nonlinearity in plunge and plunge motion
GJ	torsional stiffness
l	span length of wing
L_a	lift force about elastic axis
$LCO(s)$	limit cycle oscillation(s)
m	wing mass per unit length
M_a	pitching moment about elastic axis
r_α	radius of gyration about elastic axis
U	free-stream velocity
U_Λ	non-dimensional velocity
$U_{\Lambda L}$	non-dimensional linear flutter speed
x_α	non-dimensional distance from elastic axis to center of mass
β_ξ, β_α	constants in nonlinear terms
γ_ξ, γ_α	constants in nonlinear terms
ζ_ξ, ζ_α	viscous damping ratios in plunge and pitch
$\phi(\tau)$	Wagner's function
ϕ_h	first plunge mode shape function
ϕ_α	first pitch mode shape function
ω_h, ω_α	natural frequencies in plunge and pitch
$\overline{\omega}$	frequency ratio, ω_h/ω_θ

Appendix A

The coefficients appear in Eqs. (16)-(17) and (19)-(20) are given below

$$c_1 = \int_0^1 \left[\frac{d^2\phi_h}{d\eta^2}\right]^2 d\eta \quad c_4 = \int_0^1 [\phi_\alpha]^2 d\eta \quad c_7 = \frac{b_\Lambda}{l}\int_0^1 \frac{d\phi_\alpha}{d\eta}\phi_h d\eta \quad c_{10} = \frac{b_\Lambda}{l}\int_0^1 \frac{d\phi_h}{d\eta}\phi_\alpha d\eta \quad c_{13} = \frac{b_\Lambda^2}{l^2}\int_0^1 \frac{d^2\phi_\alpha}{d\eta^2}\phi_\alpha d\eta$$

$$c_2 = \int_0^1 \left[\frac{d\phi_\alpha}{d\eta}\right]^2 d\eta \quad c_5 = \int_0^1 \phi_h\phi_\alpha d\eta \quad c_8 = \frac{b_\Lambda^2}{l^2}\int_0^1 \frac{d^2\phi_h}{d\eta^2}\phi_h d\eta \quad c_{11} = \frac{b_\Lambda}{l}\int_0^1 \frac{d\phi_\alpha}{d\eta}\phi_\alpha d\eta$$

$$c_3 = \int_0^1 [\phi_h]^2 d\eta \quad c_6 = \frac{b_\Lambda}{l}\int_0^1 \frac{d\phi_h}{d\eta}\phi_h d\eta \quad c_9 = \frac{b_\Lambda^2}{l^2}\int_0^1 \frac{d^2\phi_\alpha}{d\eta^2}\phi_h d\eta \quad c_{12} = \frac{b_\Lambda^2}{l^2}\int_0^1 \frac{d^2\phi_h}{d\eta^2}\phi_\alpha d\eta$$

The coefficients of Eqs. (21) and (22) are given below

$$a_1 = c_3\left(1 + \frac{C_L \cos^2\Lambda}{2\pi\mu}\right)$$

$$a_2 = c_5\left(x_\alpha - \frac{a_\Lambda}{2\pi\mu}C_L \cos^2\Lambda\right)$$

$$a_3 = c_3\zeta_\xi\left(\frac{\bar\omega}{U^*}\right) + \frac{c_3}{2\pi\mu}C_L \cos^2\Lambda\left(1 - \psi_1 - \psi_2\right) + \frac{c_6}{2\pi\mu}C_L \sin 2\Lambda$$

$$a_4 = \frac{c_5}{2\pi\mu}C_L \cos^2\Lambda\left[1 + 2\left(\tfrac{1}{2} - a_\Lambda\right)\left(1 - \psi_1 - \psi_2\right)\right] - \frac{c_7}{2\pi\mu}C_L \sin 2\Lambda$$

$$a_5 = \frac{c_3}{\pi\mu}C_L \cos^2\Lambda\left(\psi_1\varepsilon_1 + \psi_2\varepsilon_2\right) + \frac{c_6}{2\pi\mu}C_L \sin 2\Lambda + \frac{c_8}{2\pi\mu}C_L \sin^2\Lambda$$

$$a_6 = \frac{c_5}{\pi\mu}C_L \cos^2\Lambda\left[1 - \psi_1 - \psi_2 + \left(\tfrac{1}{2} - a_\Lambda\right)\left(\psi_1\varepsilon_1 + \psi_2\varepsilon_2\right)\right] + \frac{c_7}{2\pi\mu}C_L \sin 2\Lambda\left(\tfrac{1}{2} - a_\Lambda\right)\left(1 - \psi_1 - \psi_2\right)$$

$$+ \frac{c_7}{4\pi\mu}C_L \sin 2\Lambda - \frac{c_9}{2\pi\mu}C_L \sin^2\Lambda\, a_\Lambda$$

$$a_7 = \frac{1}{\pi\mu}C_L \cos^2\Lambda\left[c_5\psi_1\varepsilon_1 - c_5\psi_1\varepsilon_1^2\left(\tfrac{1}{2} - a_\Lambda\right) + c_7\psi_1\varepsilon_1\left(\tfrac{1}{2} - a_\Lambda\right)\tan^2\Lambda\right]$$

$$a_8 = \frac{1}{\pi\mu}C_L \cos^2\Lambda\left[c_5\psi_{28}\varepsilon_2 - c_5\psi_2\varepsilon_2^2\left(\tfrac{1}{2} - a_\Lambda\right) + c_7\psi_2\varepsilon_2\left(\tfrac{1}{2} - a_\Lambda\right)\tan^2\Lambda\right]$$

$$a_9 = -\frac{1}{\pi\mu}C_L \cos^2\Lambda\left(c_3\psi_1\varepsilon_1^2 - c_6\psi_1\varepsilon_1 \tan\Lambda\right)$$

$$a_{10} = -\frac{1}{\pi\mu}C_L \cos^2\Lambda\left(c_3\psi_2\varepsilon_2^2 - c_6\psi_2\varepsilon_2 \tan\Lambda\right)$$

$$a_{11} = c_3 \left(\frac{\bar{\omega}}{U^*} \right)^2$$

$$a_{12} = \frac{1}{\pi\mu} C_L \cos^2\Lambda \left[c_3\xi - c_5 \left(\tfrac{1}{2} - a_\Lambda \right)\alpha \right]_{\tau=0}$$

$$b_1 = c_5 \left(\frac{x_\alpha}{r_\alpha^2} - \frac{a_\Lambda}{2\pi\mu r_\alpha^2} C_L \cos^2\Lambda \right)$$

$$b_2 = c_4 \left[1 + \frac{1}{2\pi\mu r_\alpha^2} C_L \cos^2\Lambda \left(\tfrac{1}{8} + a_\Lambda^2 \right) \right]$$

$$b_3 = -\frac{c_5}{\pi\mu r_\alpha^2} (1 + 2a_\Lambda) C_L \cos^2\Lambda \left(1 - \psi_1 - \psi_2 \right) - \frac{c_{10}}{2\pi\mu r_\alpha^2} C_L \sin 2\Lambda\, a_\Lambda \left[+ \left(\psi_1\varepsilon_1 + \psi_2\varepsilon_2 \right)(1/2 - a) \right]$$

$$b_4 = c_3 \left[\zeta_\alpha \left(\frac{1}{U^*} \right) - \frac{1}{\pi\mu r_\alpha^2} \left(\tfrac{1}{4} - a_\Lambda^2 \right) C_L \cos^2\Lambda \left(1 - \psi_1 - \psi_2 \right) + \frac{1}{2\pi\mu r_\alpha^2} \left(\tfrac{1}{2} - a_\Lambda \right) C_L \cos^2\Lambda \right]$$
$$\quad + \frac{c_{11}}{2\pi\mu r_\alpha^2} \left(\tfrac{1}{8} + a_\Lambda^2 \right) C_L \sin 2\Lambda$$

$$b_5 = -\frac{c_5}{\pi\mu r_\alpha^2} \left(\tfrac{1}{2} + a_\Lambda \right) C_L \cos^2\Lambda \left(\psi_1\varepsilon_1 + \psi_2\varepsilon_2 \right) - \frac{c_{10}}{\pi\mu r_\alpha^2} C_L \sin 2\Lambda \left(\tfrac{1}{2} + a_\Lambda \right) - \frac{c_{12}}{2\pi\mu r_\alpha^2} C_L \sin^2\Lambda\, a_\Lambda$$

$$b_6 = \frac{c_3}{\pi\mu r_\alpha^2} \left(\tfrac{1}{2} + a_\Lambda \right) C_L \cos^2\Lambda \left[1 - \psi_1 - \psi_2 + \left(\tfrac{1}{2} + a_\Lambda \right) \left(\psi_1\varepsilon_1 + \psi_2\varepsilon_2 \right) \right] + \frac{c_{11}}{8\pi\mu r_\alpha^2} C_L \sin 2\Lambda$$
$$\quad - \frac{c_{11}}{2\pi\mu r_\alpha^2} \left(\tfrac{1}{4} - a_\Lambda^2 \right) C_L \sin 2\Lambda \left(1 - \psi_1 - \psi_2 \right) - \frac{c_{11}}{4\pi\mu r_\alpha^2} C_L \sin 2\Lambda\, a_\Lambda + \frac{c_{13}}{2\pi\mu r_\alpha^2} \left(\tfrac{1}{8} + a_\Lambda^2 \right) C_L \sin^2\Lambda$$

$$b_7 = -\frac{1}{\pi\mu r_\alpha^2} \left(\tfrac{1}{2} + a_\Lambda \right) C_L \cos^2\Lambda \left[c_5\psi_1\varepsilon_1 - c_4\psi_1\varepsilon_1^2 \left(\tfrac{1}{2} - a_\Lambda \right) + c_{11}\psi_1\varepsilon_1 \left(\tfrac{1}{2} - a_\Lambda \right)\tan\Lambda \right]$$

$$b_8 = -\frac{1}{\pi\mu r_\alpha^2} \left(\tfrac{1}{2} + a_\Lambda \right) C_L \cos^2\Lambda \left[c_5\psi_2\varepsilon_2 - c_4\psi_2\varepsilon_2^2 \left(\tfrac{1}{2} - a_\Lambda \right) + c_{11}\psi_2\varepsilon_2 \left(\tfrac{1}{2} - a_\Lambda \right)\tan\Lambda \right]$$

$$b_9 = \frac{1}{\pi\mu r_\alpha^2} \left(\tfrac{1}{2} + a_\Lambda \right) C_L \cos^2\Lambda \left[c_5\psi_1\varepsilon_1^2 - c_{10}\psi_1\varepsilon_1 \tan\Lambda \right]$$

$$b_{10} = \frac{1}{\pi\mu r_\alpha^2} \left(\tfrac{1}{2} + a_\Lambda \right) C_L \cos^2\Lambda \left[c_5\psi_2\varepsilon_2^2 - c_{10}\psi_2\varepsilon_2 \tan\Lambda \right]$$

$$b_{11} = c_4 \left(\frac{1}{U^*} \right)^2$$

$$b_{12} = \frac{1}{\pi\mu r_\alpha^2} \left(\tfrac{1}{2} + a_\Lambda \right) C_L \cos^2\Lambda \left[c_5\xi + c_4 \left(\tfrac{1}{2} - a_\Lambda \right)\alpha \right]_{\tau=0}$$

Appendix B

The coefficients $k_1, k_2, \ldots, k_{10}$ and $m_1, m_2, \ldots, m_{10}$ are given below

$k_1 = (c_3 d_2 - c_2 d_3)/j$ $k_2 = (c_4 d_2 - c_2 d_4)/j$ $k_3 = (c_5 d_2 - c_2 d_5)/j$ $k_4 = (c_6 d_2 - c_2 d_6)/j$

$k_5 = (c_7 d_2 - c_2 d_7)/j$ $k_6 = (c_8 d_2 - c_2 d_8)/j$ $k_7 = (c_9 d_2 - c_2 d_9)/j$ $k_8 = (c_{10} d_2 - c_2 d_{10})/j$

$k_9 = c_{11} d_2 / j$ $k_{10} = -d_{11} c_2 / j$ $m_1 = (c_3 d_2 - c_2 d_3)/j$ $m_2 = (c_4 d_2 - c_2 d_4)/j$

$m_3 = (c_5 d_2 - c_2 d_5)/j$ $m_4 = (c_6 d_2 - c_2 d_6)/j$ $m_5 = (c_7 d_2 - c_2 d_7)/j$ $m_6 = (c_8 d_2 - c_2 d_8)/j$

$m_7 = (c_9 d_2 - c_2 d_9)/j$ $m_8 = (c_{10} d_2 - c_2 d_{10})/j$ $m_9 = c_{11} d_2 / j$ $m_{10} = -d_{11} c_2 / j$

where $j = c_1 d_2 - c_2 d_1$